JOURNAL OF COMPUTATIONAL PHYSICS 43, 260–267 (1981)

A Comparison of Numerical Solutions of Convective and Divergence Forms of the Navier–Stokes Equations for the Driven Cavity Problem

MURLI M. GUPTA

Department of Mathematics, The George Washington University, Washington, D.C. 20052

Received February 17, 1981

The two-dimensional Navier-Stokes equations governing the steady flow of a viscous incompressible fluid are usually written in the convective or the divergence form. There is a continuing controversy in the literature about the superiority of the divergence form over the convective form. The effect of central and upwind differencing is examined on each of these formulations and it is concluded that none of these formulations has absolute superiority over the other. The problem of the driven cavity is taken as a test model.

1. INTRODUCTION

The two-dimensional Navier–Stokes equations have been solved by many researchers and a variety of finite difference, finite element and other techniques have been proposed in the literature. Many researchers, especially those using finite difference methods, have concentrated on solving the convective form of the Navier–Stokes equations while others have solved the divergence formulation, which automatically satisfies the principle of mass conservation. Some of these solutions, especially for small Reynolds numbers, have shown good agreement. However, there remains much disagreement over the characteristics of the numerical solutions for moderate to large Reynolds numbers.

In this paper we examine the numerical solutions of both convective and divergence forms of the Navier–Stokes equations through the use of central and upwind differencing of the two formulations. The numerical solutions of the four finite difference approximations are obtained under identical conditions and the behaviour of these solutions is critically analyzed.

2. THE FORMULATIONS

The Navier–Stokes equations governing the steady flow of an incompressible viscous fluid may be written in the nondimensional forms

$$\nabla^2\omega - R(u\omega_x + v\omega_y) = 0, \tag{1}$$

0021-9991/81/100260–08$02.00/0

$$\nabla^2\omega - R((u\omega)_x + (v\omega)_y) = 0. \tag{2}$$

Here Eq. (1) is the convective (advective) form of the vorticity transport equation. Equation (2) is the divergence (conservative) form, which automatically satisfies the principle of mass conservation ($u_x + v_y = 0$). The velocities u, v are related to the streamfunction ψ and vorticity ω through the relations

$$\begin{aligned} u &= \psi_y, \qquad v = -\psi_x; \\ \omega &= v_x - u_y = -\nabla^2\psi. \end{aligned} \tag{3}$$

We consider the problem of the driven cavity [1–3, 5–7, 9] as a model. The bounday conditions are those of no-slip on the boundary of the square ($0 \leqslant x, y \leqslant 1$) (see Fig. 1):

$$\begin{aligned} &\psi = 0, \quad \psi_y = -1 \quad \text{on the sliding wall } y = 1, \\ &\psi = 0, \quad \psi_n = 0 \quad \text{on the stationary walls.} \end{aligned} \tag{4}$$

The square cavity is covered by a set of $(n+1) \times (n+1)$ mesh points uniformly spaced with mesh spacing $h = 1/n$. Equations (1), (2) may be discretized by using central difference approximations for all derivatives. The resulting schemes are called CDC (Central Difference Convective Scheme) and CDD (Central Difference Divergence Scheme), respectively. The other possibility is to use central differences for $\nabla^2\omega$ and one-sided differences for the first order derivative in Eqs. (1), (2) thus yielding UDC (Upwind Difference Convective Scheme) and UDD (Upwind Difference Divergence Scheme), respectively. For detailed description of these schemes, see [1, 5–7].

After the vorticity equation (1) or (2) has been approximated by a finite difference scheme at each mesh point, the resulting algebraic equations may be written in a

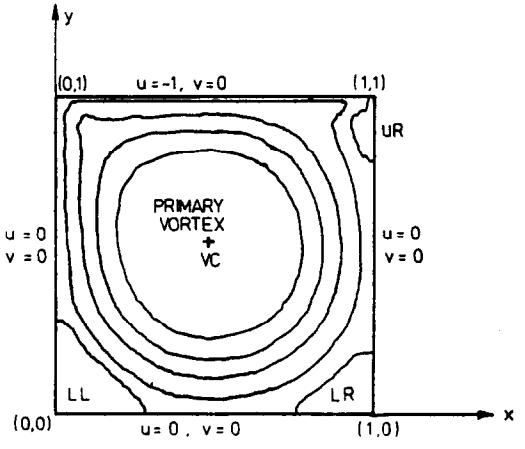

FIGURE 1

matrix form with non-symmetric and non-constant coefficient matrix. This matrix is diagonally dominant for the upwind schemes UDC, UDD but not diagonally dominant for the central schemes CDC, CDD. The matrix equation is solved in conjunction with the usual second order approximation of the streamfunction equation $\nabla^2\psi = -\omega$ which yields a symmetric, positive definite coefficient matrix. The coupling is provided by the vorticity values on the boundaries of the cavity which are approximated by a second order approximation called the (2, 1) formula in [6, 7]. As an example, on the left boundary $x = 0$ we write

$$\omega_{0j} = -h^{-2}[4\psi_{1,j} - \tfrac{1}{2}\psi_{2,j}], \qquad 1 \leqslant j \leqslant n-1. \tag{5}$$

3. The Numerical Solutions

The numerical solution of the coupled algebraic equations is obtained using an outer iterative procedure described in detail in [6, 7]. At each outer iteration the algebraic equations corresponding to (1)–(2) and (3) are solved by direct solvers such as LEQT1B from the IMSL package and MA28 from the Harwell package [4]. The damping parameters are used according to the discussion in [6, 7] and the outer iterations are continued until the successive ψ, ω iterates differ by an amount smaller than 10^{-4} at each mesh point.

We obtained the numerical solutions of the four finite difference schemes (CDC, UDC, CDD, UDD) for several Reynolds numbers in the range 1–5000 with mesh sizes $h = 1/20$, $1/32$. For small Reynolds numbers all schemes converged quite satisfactorily. When the Reynolds number was increased, two of these schemes exhibited convergence problems. The solutions of CDC were not obtained beyond $R = 1000$ as these solutions already became incorrect, both qualitatively and quantitatively [7]. The outer iterative procedure with UDD exhibited an oscillatory behaviour for $R > 1000$ with single precision arithmetic. With double precision, however, monotonic convergence could be achieved for UDD for $R = 5000$. On the other hand, UDC and CDD converged for all values of R. We note at this point that the UDD scheme is computationally more complex to code than are any of the other schemes.

In order to compare the effect of the four finite difference schemes, we obtained their solutions under identical conditions. The values of streamfunction at the centre of primary vortex ($\psi_{VC} = \max_{i,j}|\psi_{i,j}|$) are given in Table I.

For small Reynolds numbers, the central difference schemes CDC, CDD yield approximately the same values. For larger Reynolds numbers, CDD yields better values compared to the CDC solutions. The CDC solutions begin to deteriorate and exhibit oscillatory behaviour in the vorticity values on the sliding wall $y = 1$ for $R \geqslant 500$ [7]. A comparison of the upwind solutions shows that UDC yields better solutions for small R. For large values of R, both UDC and UDD suffer from the effects of false diffusion [3, 10] and yield approximately similar solutions. The values

TABLE I

Strength of Primary Vortex ψ_{VC} $(h = 1/20)$

R	CDC	UDC	CDD	UDD
1	0.0995	0.0995	0.0995	0.0994
10	0.0993	0.0998	0.0994	0.0984
100	0.0969	0.1001	0.1015	0.0918
500	0.0647	0.0775	0.1024	0.0729
1000	0.0336	0.0599	0.0972	0.0626
5000	—	0.0405	0.0727	0.0402

TABLE II

Value of Vorticity at the Vortex Centre ω_{VC} $(h = 1/20)$

R	CDC	UDC	CDD	UDD
1	3.0154	3.0162	3.0154	3.0109
10	3.0010	3.0094	3.0040	2.9591
100	3.3636	3.1250	3.0544	2.7880
500	1.9048	2.6757	2.0504	1.5876
1000	40.6211	2.6299	1.7451	1.2649
5000	—	1.2415	1.1306	0.5800

TABLE III

Drag on the Moving Wall C_D

R	CDC	UDC	CDD	UDD
1	25.4428	25.4190	25.4422	25.4853
10	2.5495	2.5264	2.5474	2.5913
100	0.2950	0.2669	0.2788	0.3080
500	0.1095	0.0762	0.0811	0.0922
1000	0.0736	0.0480	0.0501	0.0565
5000	—	0.0137	0.0150	0.0161

of vorticity at the vortex centre are given in Table II. These values confirm the observations made above.

We also give the value of drag coefficient on the sliding wall defined by

$$C_D = \frac{2}{R}\int_0^1 \omega(s, 1)\, ds = \frac{2}{R}\bar{F}, \tag{6}$$

where $\bar{F}$ is the value of the shear force on the sliding wall [6]. The integral here is

obtained by using trapezoidal rule over the 21 mesh points on the sliding wall. The values of C_D are given in Table III.

It is noted that for small R, CDC and CDD yield similar values of C_D. It is also noted that in comparison to the CDD solutions, UDC yields a lower values of C_D whereas UDD yields a higher values of C_D.

A few authors have mentioned the appearance of a third secondary vortex in the upper right corner of the cavity near the upstream singular point. DeVahl Davis and Mallinson [3] observed this separation for $R = 2000$ with CDD and a non-uniform 31×31 mesh. Olson and Tuann [9] used a finite element method and discovered the appearance of such a vortex at $R = 1500$. In a recent work, Chen *et al.* [2] also reported the apearance of such a secondary vortex at $R = 2000$ using a finite analytic method with 61×61 mesh. In our computations, such a vortex was observed for $R \geqslant 1000$ ($h = 1/20$). However, the separation near the upstream singular corner was only observed with CDD. For $R = 1000$ the centre of this secondary vortex was found to be $(\bar{x}, \bar{y})$, where $\bar{x} \in (0.95, 1.0)$ and $\bar{y} = 0.90$. For $R = 2000$ and 5000, the centre was $(0.95, 0.90)$ with $\psi_{VC} = -0.0016$, $\omega_{VC} = -6.1036$ for $R = 2000$ and $\psi_{VC} = -0.0033$, $\omega_{VC} = -7.1894$ for $R = 5000$.

It is instructive to examine the behaviour of vorticity values on the right wall ($x = 1$) with CDD; see Fig. 2. For small values of R ($\leqslant 100$), the values of $\omega(1, y)$ increase monotonically from $-\infty$ at $y = 1$ to 0 at the separation point ($y \simeq 0.07$) of the secondary vortex in the lower right corner LR. At $R = 200$, this curve has a point of inflexion near $y = 0.7$. For larger values of R, the values of $\omega(1, y)$ fail to increase monotonically from $-\infty$ at $y = 1$ to 0 at the lower separation point. Indeed, the oscillation near $y = 0.9$ becomes large enough for $R \geqslant 1000$, thereby causing the appearance of the third secondary vortex near the upstream singular corner.

At this point it is not clear whether the appearance of this secondary vortex is a sign of better accuracy or inaccuracy of the CDD solutions. The CDC solutions exhibit oscillatory behaviour in the vorticity values on the sliding wall for large Reynolds numbers [7]. The CDD solutions did not exhibit such oscillations; however, the behaviour of $\omega(1, y)$ (see Fig. 2) may be a sign of forthcoming trouble for large values of R.

It is noted that DeVahl Davis and Mallinson [3], who reported the appearance of the third secondary vortex for the first time, used the CDD in their computations. Olson and Tuann [9] also observed such a vortex in their finite element calculations. However, Olson and Tuann [9] obtained their solutions by prescribing $u = v = 0$ at the singular corners which forced the vorticity at (0, 1) and (1, 1) to be 0. In reality vorticity at these points should be infinite. They set $u = -1$, $v = 0$ at all other nodes on the sliding wall $y = 1$, and allowed the tangential velocity u to vary cubically from 0 at the corner to -1 at the next node point [9, p. 126]. In such circumstances the vorticity values near the singular corners ought not to be considered reliable.

In a recent paper Gupta *et al.* [8] obtained asymptotic expressions for ψ, ω, u, v in the neighborhood of singular corners and discovered that the vorticity values on the stationary walls ($x = 0$, $x = 1$) are very sensitive to the inaccuracies of the numerical solution processes. We believe that the appearance of the third corner vortex in the

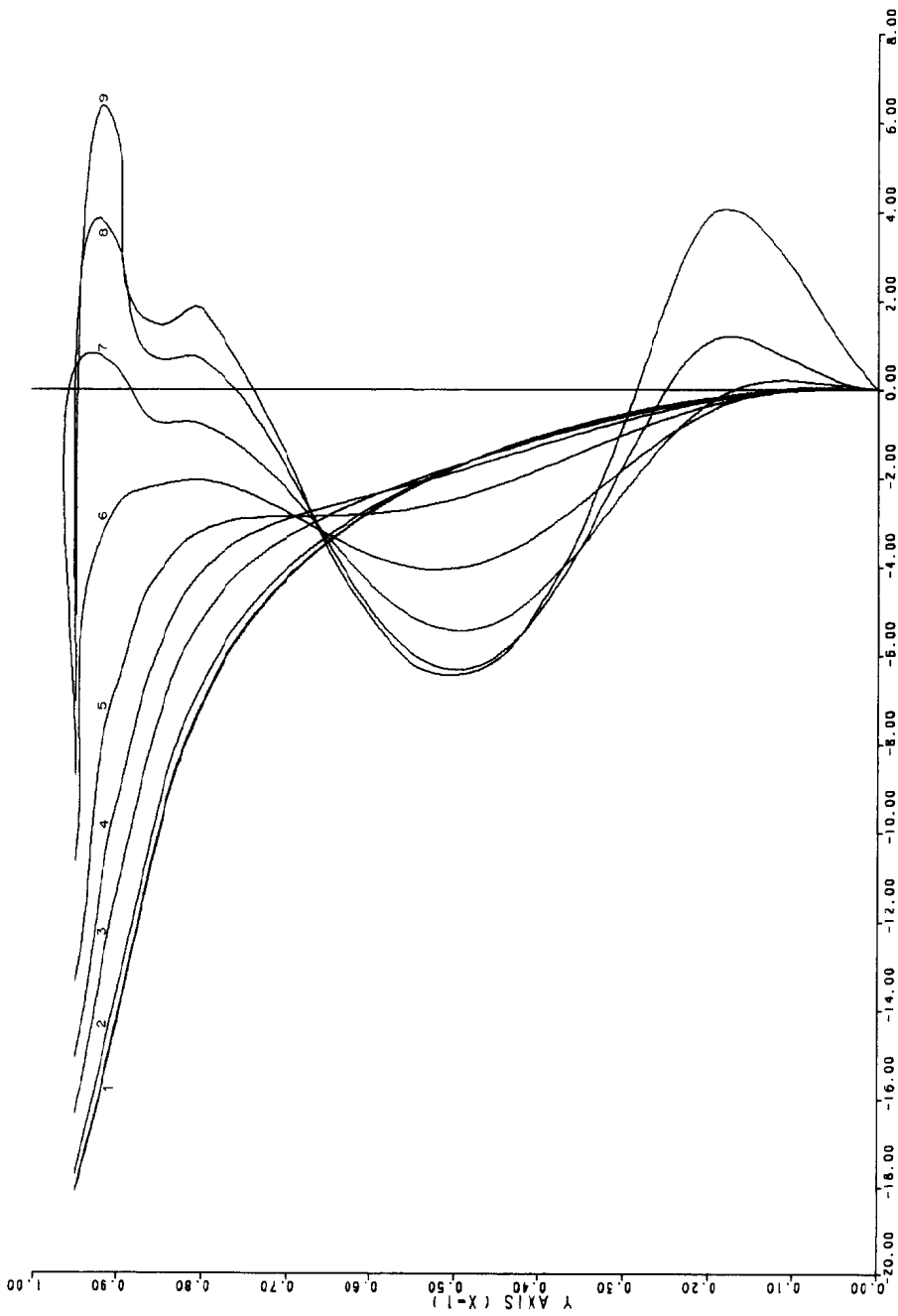

FIG. 2. Vorticity values on right wall (CDD). Values of R are: (1) 0, 1; (2) 10; (3) 50; (4) 100; (5) 200; (6) 500; (7) 1000; (8) 2000; (9) 5000.

solutions of [2, 9] ought to be investigated further to see if this is introduced solely by the particular discretization or computational procedure.

Finally we note that the secondary vortices in the lower corners exhibited a shrinking behaviour as R increased with both upwind (UDC, UDD) and central (CDD) schemes. With the upwind schemes, the lower right vortex (LR) disappeared at $R = 5000$ whereas the lower left (LL)vortex disappeared with CDD at $R = 5000$.

4. Conclusions

We have presented a comparison of numerical solutions which were obtained using central and upwind difference approximations of the convective as well as divergence form of the Navier–Stokes equations for the driven cavity problem. The divergence form yields solutions vastly superior to those of the convective form when central differencing is used, especially for large Reynolds numbers. However, when upwind differencing is used, the solutions of the two formulations are almost equivalent in accuracy, the convective form having a slight edge over the divergence form for small Reynolds numbers. The upwind formulation of the divergence form is computationally more complex than that of the convective form. Moreover, Gresho and Lee [10] have recently raised the question of the validity of *any* upwind solutions for large Reynolds numbers and it seems unnecessary to use the divergence form with upwind formulations.

The central difference solutions of the divergence form do not exhibit the oscillatory behaviour observed with the convective form [7]. The CDD solutions remain satisfactory for larger Reynolds numbers than do the CDC solutions. However, the CDD solutions exhibit a secondary vortex near the upstream singular corner.

It is, at present, not certain whether the appearance of such a secondary vortex is a sign of better accuracy or inaccuracy of the CDD solutions. One could conjecture, as do Gresho and Lee [10], that the appearance of such a vortex is a "signal" that the mesh is too coarse to resolve the flow correctly for the Reynolds number used. When the mesh is refined, a similar signal should be observed for higher Reynolds numbers. In support of this conjecture we note the apearance of such a signal with a uniform 21×21 mesh for $R \geqslant 1000$. In the work of DeVahl Davis and Mallinson [3] such a signal appears for $R = 2000$ with a nonuniform 31×31 mesh.

Our solutions, especially those obained for large Reynolds numbers, may not be very accurate because of the crude mesh used. However, the relative behaviour of these solutions, which were obtained under identical conditions, is believed to be representative of the general case.

References

1. J. D. Bozeman and C. Dalton, *J. Comput. Phys.* **12** (1978), 348–363.

2. C.-J. CHEN. H. NASERI-NESHAT, AND P. LI, "The Finite Analytic Method", Rep. E-CJC-1-80, The University of Iowa, Iowa City, 1980.
3. G. DEVAHL DAVIS AND G. D. MALLINSON, *Comput. and Fluids* **4** (1976), 29–43.
4. I. S. DUFF, "MA28—A set of FORTRAN Subroutines for Sparse Unsymmetric Linear Equations," Rep. AERE-R8730, AERE, Harwell, U. K., 1977.
5. M. M. GUPTA, *in* "Innovative Numerical Analysis for the Engineering Sciences" (R. Shaw, *et al.*, Ed.), pp. 277–285, Univ. Virginia Press, 1980.
6. M. M. GUPTA AND R. MANOHAR, *J. Comput. Phys.* **31** (1979), 265–288.
7. M. M. GUPTA AND R. MANOHAR, *Int. J. Numer. Methods Engrg.* **15** (1980), 557–573.
8. M. M. GUPTA, R. MANOHAR, AND B. NOBLE, *Comput. and Fluids*, in press.
9. M. D. OLSON AND S. Y. TUANN, *Comput. and Fluids* **7** (1979), 123–135.
10. P. GRESHO AND R. L. LEE, *Comput. and Fluids* **9** (1981), 223–253.